PB293-308

Report of Investigations 8335

Erosion Testing of Potential Valve Materials for Coal Gasification Systems

By J. S. Hansen, J. E. Kelley, and F. W. Wood

March 3 1849

UNITED STATES DEPARTMENT OF THE INTERIOR
Cecil D. Andrus, Secretary

BUREAU OF MINES
Roger A. Markle, Director

The work upon which this report is based was done under a cooperative agreement between the Bureau of Mines, U.S. Department of the Interior, and the U.S. Department of Energy.

This publication has been cataloged as follows:

Hansen, Jeffrey S

Erosion testing of potential valve materials for coal gasification systems / by J. S. Hansen, J. E. Kelley, and F. W. Wood. [Washington] : U.S. Dept. of the Interior, Bureau of Mines, 1979.

26 p. : ill., diagrs. ; 27 cm. (Report of investigations - Bureau Mines ; 8335)

Based on work done in cooperation with the U.S. Department of Energy.

Bibliography: p. 14-15.

1. Coal gasification. 2. Valves - Testing. I. Kelley, John E., joint author. II. Wood, F. W., joint author. III. United States. Bureau of Mines. IV. Title. V. Series: United States. Bureau of Mines. Report of investigations - Bureau of Mines ; 8335.

TN23.U7 no. 8335 622.06173

U.S. Dept. of the Int. Library

CONTENTS

ILLUSTRATIONS

TABLES

EROSION TESTING OF POTENTIAL VALVE MATERIALS FOR COAL GASIFICATION SYSTEMS

by

J. S. Hansen,[1] J. E. Kelley,[1] and F. W. Wood[2]

ABSTRACT

In support of its objective to conserve mineral resources by minimizing premature failure of materials, the Bureau of Mines conducted a cooperative study with the U.S. Department of Energy on the erosion and abrasion resistance of hard materials for valves in coal conversion systems. This report describes a newly developed erosion-testing apparatus and presents data on the erosion resistance of over 200 materials.

Erosion resistance of most metals was comparatively low. In contrast, ceramics and cermets such as B_4C, WC, SiC, Si_3N_4, and TiB_2, when fabricated to minimize porosity, displayed greater than five times the erosion resistance of metals. Coatings such as boron diffused into Mo and WC, chemical-vapor-deposited TiCN, and electrodeposited TiB_2 were highly erosion resistant if applied in thicknesses ranging from 60 to 75 µm. Erosion resistance of cemented carbides was inversely related to metal binder content.

INTRODUCTION

Beginning in 1945, the Bureau of Mines constructed a series of pilot plants to demonstrate various coal gasification technologies (12).[3] Presently, a stirred-bed, producer-gas facility (Morgas) is in operation at Morgantown, W. Va. (10), and a synthetic natural gas facility (Synthane) is in operation at Bruceton, Pa. (7). Other coal gasification investigations are underway throughout the world (2).

A general problem that has developed in coal gasification is the short wear life of valves used to transfer solids as dry bulk, slurries, or gas-borne particulates. The valves are exposed to harsh conditions: temperatures and pressures are high; gases are reactive; the coal, coal dust, char, and ash

---

[1] Metallurgist, Albany Metallurgy Research Center, Bureau of Mines, Albany, Oreg.

[2] Supervisory research physicist, Albany Metallurgy Research Center, Bureau of Mines, Albany, Oreg. (now with the Naval Air Rework Facility, Materials Engineering Division, Naval Air Station, Jacksonville, Fla.).

[3] Underlined numbers in parentheses refer to items in the list of references preceding the appendixes.

are abrasive; and condensed tars cause gritty materials to stick on wear-prone surfaces. Materials that are currently available in off-the-shelf valves have proven inadequate to the conditions. An objective of the Bureau of Mines is to conserve mineral resources by minimizing material wear losses. This study, conducted in cooperation with the U.S. Department of Energy, supports that objective.

The careful selection of available wear-resistant materials and the development of improved materials offer partial solutions to wear problems. In this regard, the Bureau of Mines conducted an investigation which included both laboratory screening of candidate materials and service testing of the more promising materials as valve parts in the Morgas gasifier. The laboratory tests in one particular wear mode, erosion, are the subject of this report. Results of other wear tests conducted in the investigation will be reported separately.

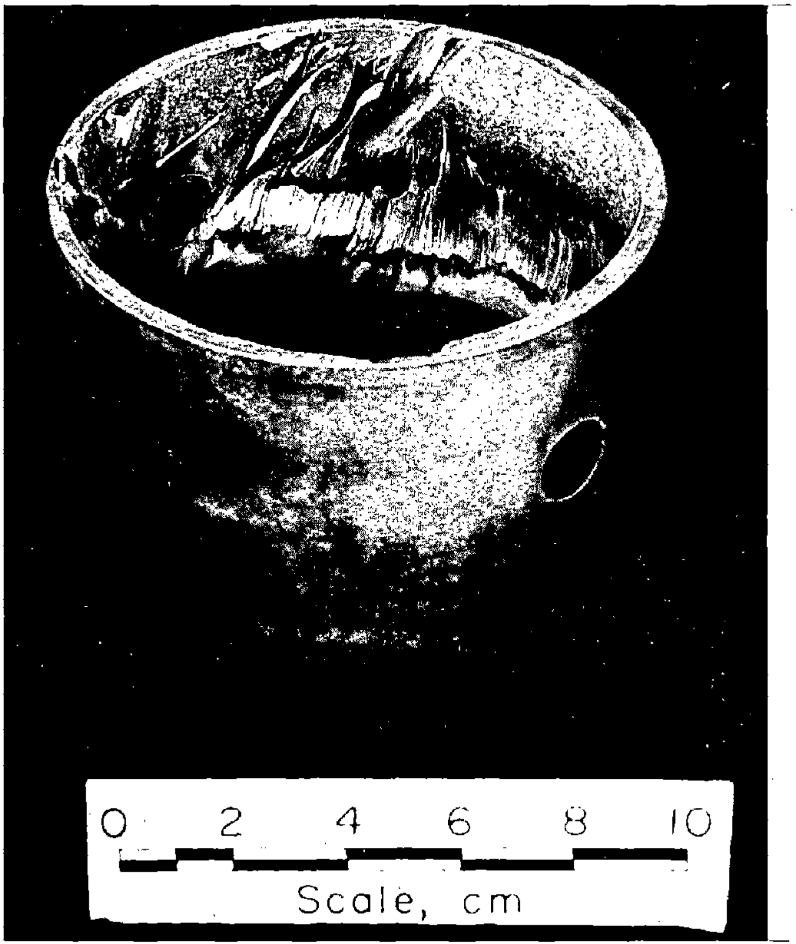

FIGURE 1. - Erosion damage to a 316 SS butterfly valve liner caused by hot, dirty product gas from the Morgas gasifier.

Erosion, according to an ASTM definition,[4] is the progressive loss of original material from a solid surface owing to mechanical interaction between that surface and a fluid, a multicomponent fluid, or impinging liquid or solid particles. The 316 stainless steel butterfly valve liner shown in figure 1 is an example of solid particle erosion in a coal gasifier. The valve, which was used to regulate gasifier pressure, was located in a product gas line of the Morgas pilot plant and eroded through in less than 40 hours of operation. Another example, an eroded ball valve which was used to seal a lock hopper at 300 psig against atmospheric pressure, is shown in figures 2 and 3. The erosion was caused after a small leak developed (possibly from an abrasive wear scar)

---

[4] Proposed by Committee G-2 for inclusion in a revision of American Society for Testing and Materials standard G40-73.

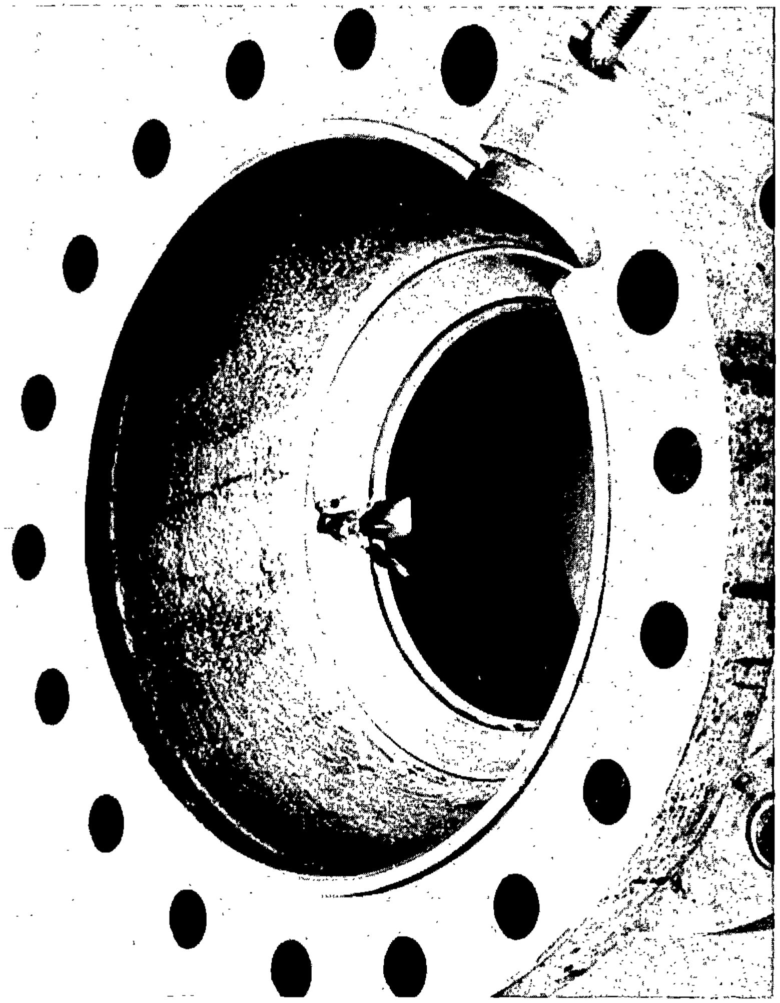

FIGURE 2. - Erosion damage to a lock hopper ball valve seat caused by a high-velocity stream through a leak.

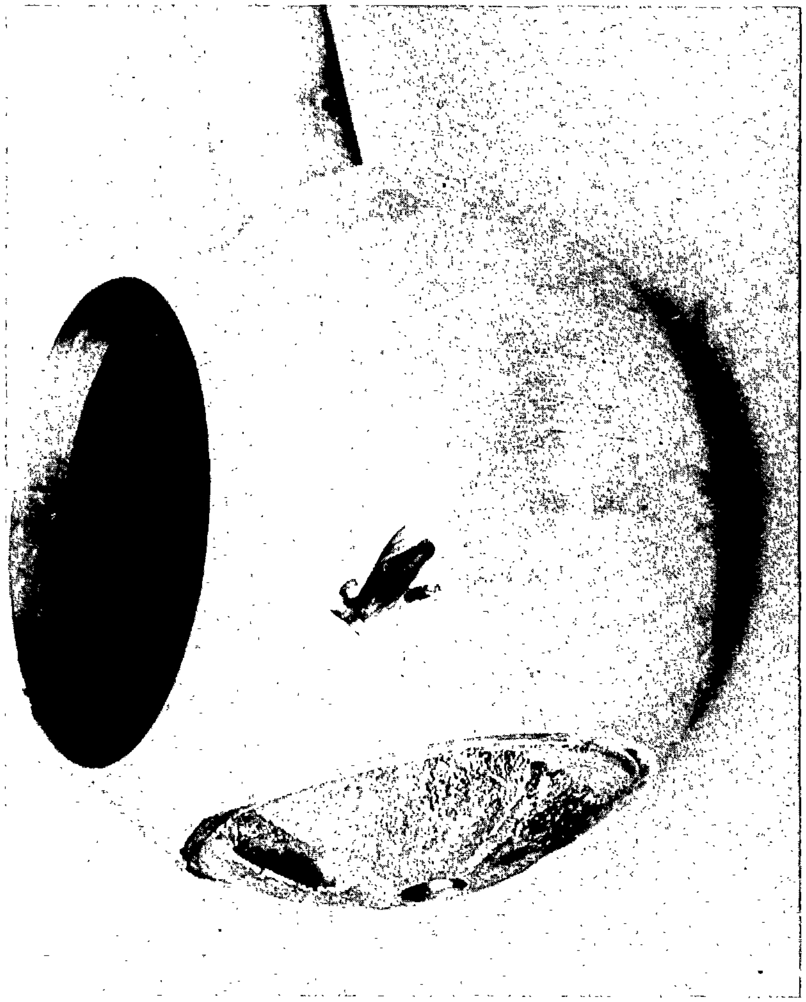

FIGURE 3. - Erosion damage to the mating ball of the equipment shown in figure 2.

and was steadily increased in size by high-velocity ash-laden gases. This type of failure is common and is known as the "wire-drawing effect."

Although previous researchers have done substantial work, erosion problems in gasifier valves and elsewhere remain formidable. The complex nature of the problem is such that a change in any one of several variables affecting erosion renders a material satisfactory in one application but unsuitable in another. (The variables are defined in appendix A.) Researchers have developed several relationships to equate the variables to physical properties (1, 6, 8-9, 11, 16-17). However, design engineers, needing materials selection guidance, have found the equations to be of little practical significance in that they apply only to narrow classes of materials, difficult-to-measure properties are involved, all variables are not accounted for in any one equation, and special tests are required for the determination of constants. Furthermore, useful published erosion data are lacking, and standard erosion tests are nonexistent.

In this study, no attempt was made to determine the causes of erosion or to improve upon established erosion models. Instead, an empirical erosion data bank has been developed.

TEST EQUIPMENT

Room-temperature erosion tests were performed by using a sandblast-type tester. The tester incorporated an S. S. White Model H Airbrasive[5] unit to mix alumina particles with a gas stream and to control the particle flow rate and velocity. The mixing was accomplished within the Airbrasive unit by a pressurized particle container mounted on a vibrator. An orifice in the container bottom controlled the flow of particles into the gas stream. The particle flux was a function of the voltage applied to the vibrator, and the velocity was a function of the gas stream pressure. All particle velocities were measured on a two-disk device described by Ruff (13).

The particle delivery nozzle was specially designed to minimize nozzle wear and to withstand high temperatures. It consisted of a molybdenum shank about 4 cm (1.6 in) long and a 1.3-cm (0.5-in) sapphire tip 0.058 cm (0.023 in) in inside diameter, which was glued into one of the shank ends. During elevated-temperature operation, the glue evaporated, but the tip remained secure because of tip and shank thermal expansion differences.

Elevated-temperature tests were done in one of two high-temperature systems. The first system (fig. 4) consisted of the Airbrasive unit, a sealed Kanthal resistance furnace, a specimen stage, a shutter to control the abrasive blast duration, and the same particle delivery nozzle that was used in room-temperature tests. A thermocouple was placed behind the specimen, and the test temperature profile was recorded. A tube to flow a simulated coal gasifier atmosphere without abrasive or to evacuate the furnace was situated next to the specimen. A reference specimen that experienced all test

---

[5] Specific brand names are used for identification and description only and do not imply endorsement by the Bureau of Mines.

conditions except the particle blast was attached to the opposite side of the specimen stage. Its purpose was to determine the degree of corrosion loss.

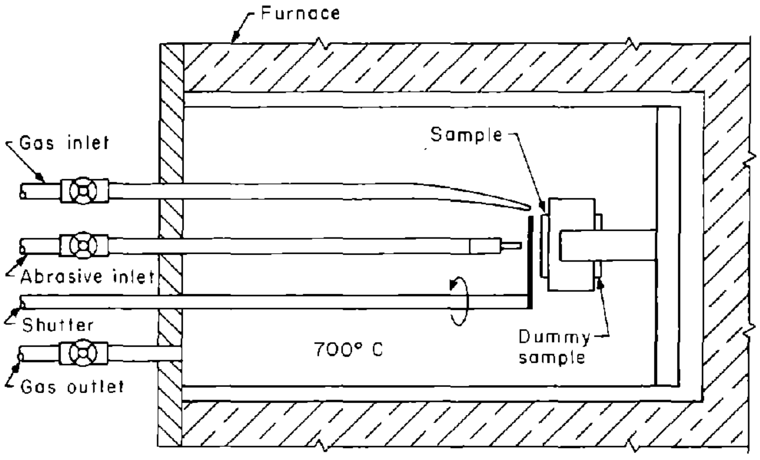

FIGURE 4. - The one-specimen, high-temperature erosion test system.

Because the one-specimen system was inadequate for the large number of materials that were to be screened, a larger apparatus capable of accommodating multiple specimens was constructed. Details are shown in figures 5 and 6. Essentially all internal equipment from the first system was duplicated in the second system, except that a multifaceted turret was used to secure 12 specimens for testing in one heating, and an infrared pyrometer was used to monitor the temperature of the impingement area. The erosion losses of reference materials, tested in both systems, were comparable.

PROCEDURE

Two test procedures were used, one for room-temperature tests and the other for elevated-temperature tests. Both procedures utilized specimens that were nominally 1.3 by 1.3 by 0.2 cm (0.5 by 0.5 by 0.063 in). Specimens were cleaned and weighed before testing. In room-temperature tests, specimens were positioned 0.952 cm (0.375 in) beneath the nozzle tip. The angle of incidence was adjusted to either 90° or 20°, and a hand-operated shutter was passed between the nozzle tip and the specimen surface. Subsequently, the particle blast was started and allowed to reach a steady state, after which the shutter was removed. The particle blast was stopped after 3 minutes, and the specimens were recleaned and reweighed.

Parameters were identical for high-temperature tests. Heating was normally done under a partial vacuum, but in some instances in which specimens were readily oxidized, heating was done under a small flow of nitrogen. When the desired test temperature was reached, a stream of nitrogen or other gas was directed to the specimen surface at a rate equal to that which flowed through the particle nozzle during a test. Specimen temperatures dropped initially but rapidly returned to normal. At steady state, a shutter was positioned between the nozzle and specimen, and the particle blast was started. As soon as the particle blast was constant, the shutter was manually removed to begin the test. The impingement area temperature rapidly dropped an average of 63° C in tests begun at 700° C, remained at about 637° C for the duration of the 3-minute test, and returned to 700° C upon the automatic test termination. Another specimen was indexed under the nozzle in the 2-minute period that elapsed prior to the next test. The procedure was repeated for

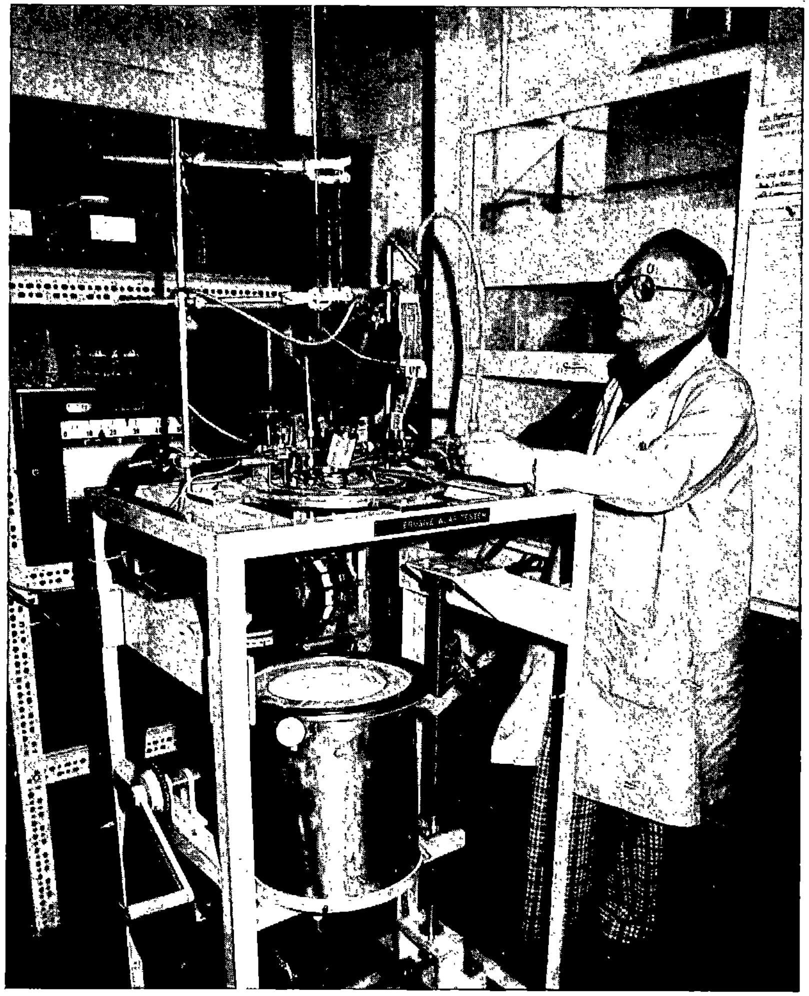

FIGURE 5. - The multispecimen, high-temperature erosion test system.

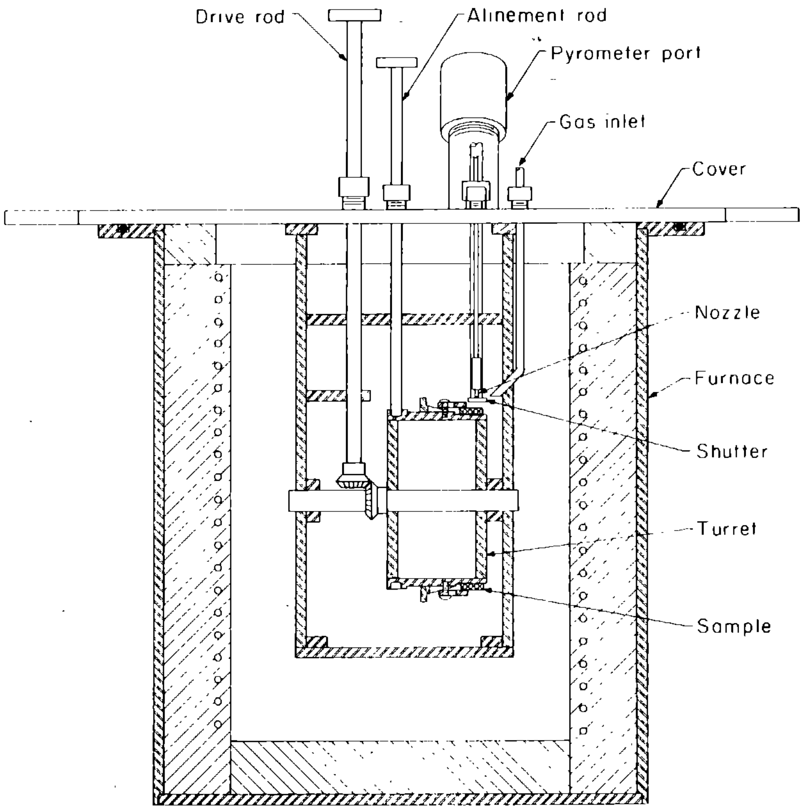

FIGURE 6. - Cross section of the internals of the multispecimen, high-temperature erosion test system showing the 12-faceted turret with specimens affixed for 90° impingement.

the remaining specimens, and at the conclusion, the furnace contents were cooled under nitrogen. The tested specimens were recleaned, reweighed, and checked for excessive oxidation, cracking, and spalling.

A control and computation procedure was developed to organize both the room-temperature and high-temperature weight loss data and to reduce an error that resulted from particle flux variations caused by the Airbrasive unit vibratory feeder. In the procedure, three Haynes Stellite alloy 6B wrought standards from a single source were run at equal intervals with each set of nine specimens. The erosion tester was adjusted to keep the volume loss of the standards within 10 pct of a value established from preliminary tests. The standard volume loss was 0.00146 cm^3 at room temperature and 0.00178 cm^3 at 700° C, both at a 90° impingement angle, and 0.00219 cm^3 at room temperature and a 20° impingement angle. A series of tests showed that when the Stellite 6B erosion losses deviated from these values, the erosion loss of the specimens deviated a proportional amount; that is, the ratio of the specimen volume loss to the Stellite 6B erosion loss remained constant over a range of particle fluxes. Therefore, this ratio was chosen as the means by which all materials were ranked and is referred to hereafter as the relative erosion factor (REF).

TEST PRECISION

The reference specimens that were run with each elevated-temperature test in the first erosion tester had weight losses due to oxidation or corrosion of less than 1.5 pct of total weight in most cases. Some exceptions were Beta III Ti, which gained 15 pct; 316 SS, which gained 4.2 pct; and some of the SiC and WC materials, which also gained several percent. Because the weight changes due to oxidation were generally low, reference specimens were not run in the improved erosion tester.

The erosion factor values referred to in the "Results" section of the report are the mean of five tests. One standard deviation of a set of five tests was typically within 10 pct of the mean. Variations were higher in some of the most erosion-resistant materials, such as K-714 with 30.24 pct or Noroc-33 with 21.5 pct, because weighing precision closely approached the total weight loss of these specimens. Additional error was caused by the change in impingement angle with time that resulted when the geometry in portions of the developing erosion pit was altered as the test proceeded. This error was greatest in specimens that lost large volumes.

RESULTS AND DISCUSSION

A large number of materials were subjected to the same test conditions. The relative erosion factors, chemical compositions, and manufacturing methods are listed in appendix B. For further clarity, a representative portion of the information is graphically presented in figures 7 through 12, according to material type.

As shown in figure 7, most metals and metallic alloys, except tungsten and molybdenum, had nearly the same room-temperature REF values with a 90° impingement. At best, only a 30-pct improvement over Stellite 6B was evident.

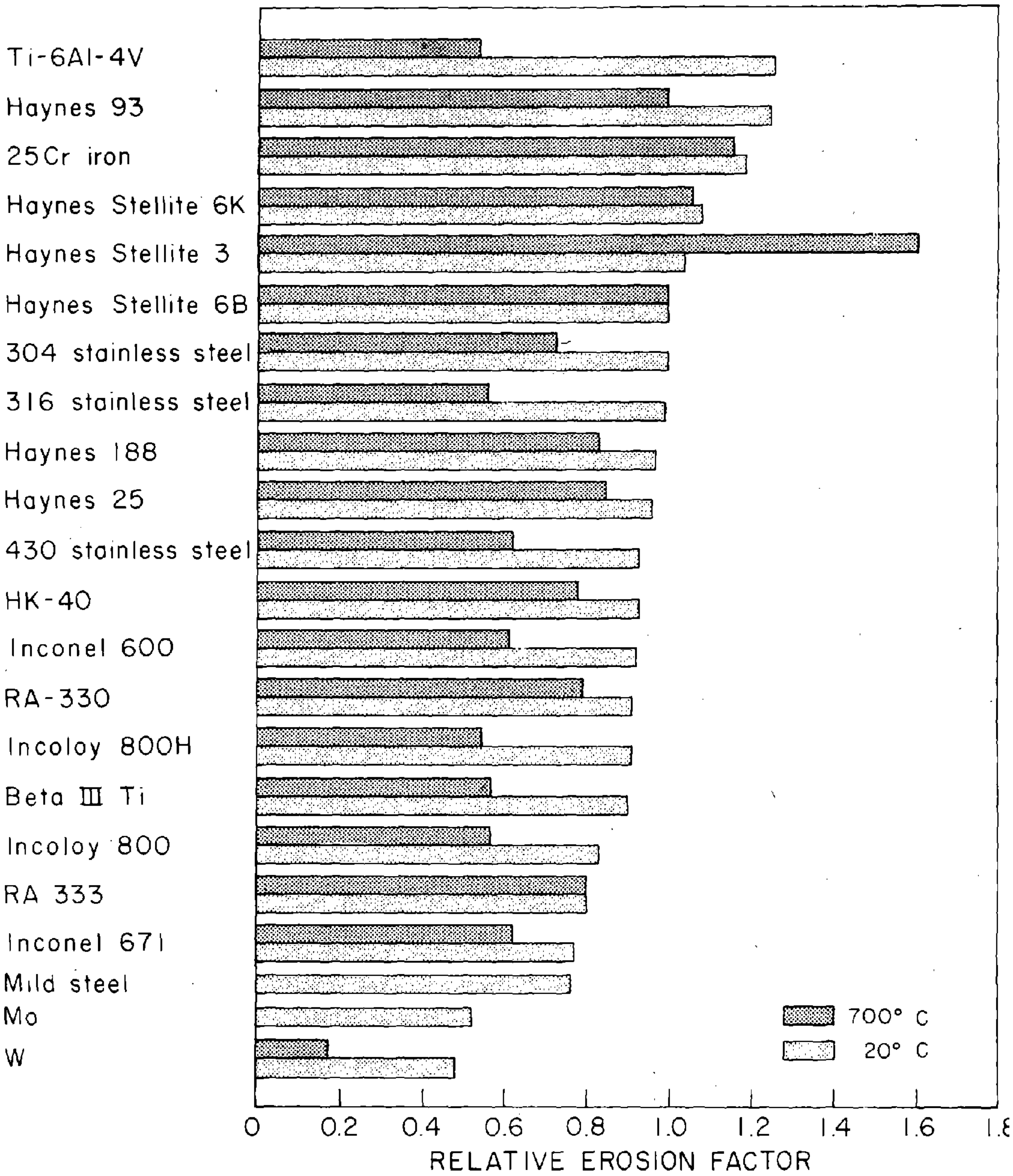

FIGURE 7. - REF's of commercially available metals (90° impingement).

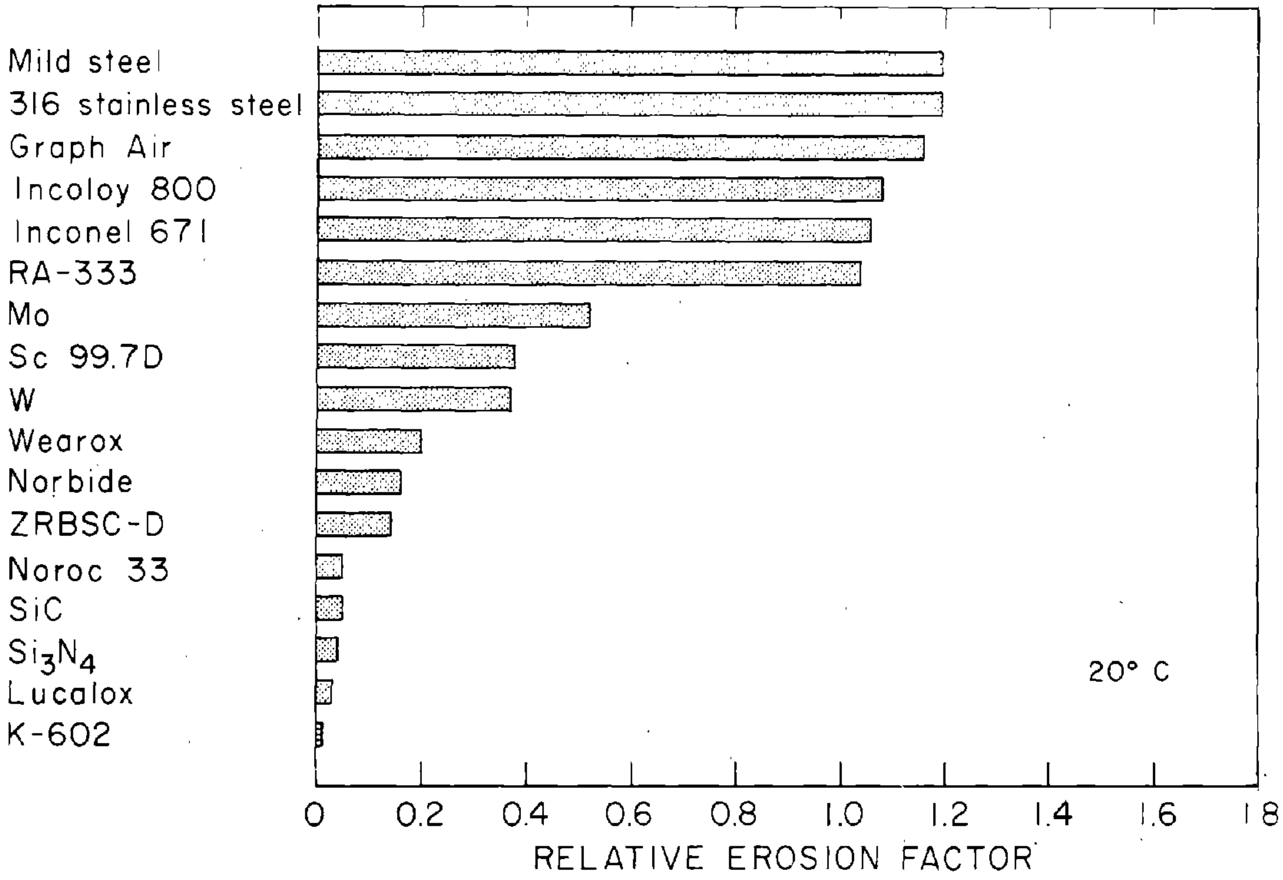

FIGURE 8. - REF's of several metals and ceramics (20° impingement).

From figure 8, all metallic alloys, except tungsten and molybdenum, again had similar erosion resistances at a 20° impingement, but in addition all had lower REF values.

Many alloys eroded more at 700° C than at room temperature, but a few eroded less. No explanation for the mixed high-temperature behavior was apparent, although others have noted similar results. Young (19), using 5-μm particles and a 52-m/sec particle velocity, found erosion penetration was markedly less at 500° C than at 25° C in tests on several stainless steels and high-Ni-Cr alloys. However, with a 50-μm particle size, erosion penetration was slightly more at 500° C than at 25° C on most of the same materials. Young postulated that the chromium in the materials rapidly formed an adherent, self-healing, and protective oxide barrier that had an erosion resistance greater than that of the underlying metal. Presumably, the barrier was more protective against bombardment by the 5-μm particles than against the 50-μm particles because the larger particles were capable of causing more damage at an equal velocity. Smeltzer (17) found a related behavior in 2024 Al, Ti-6Al-4V, and 17-7 PH stainless steel. Because the erosion was greater at high impingement angles than at lower angles, Smeltzer also surmised that a ceramic film was protecting the substrate material underneath.

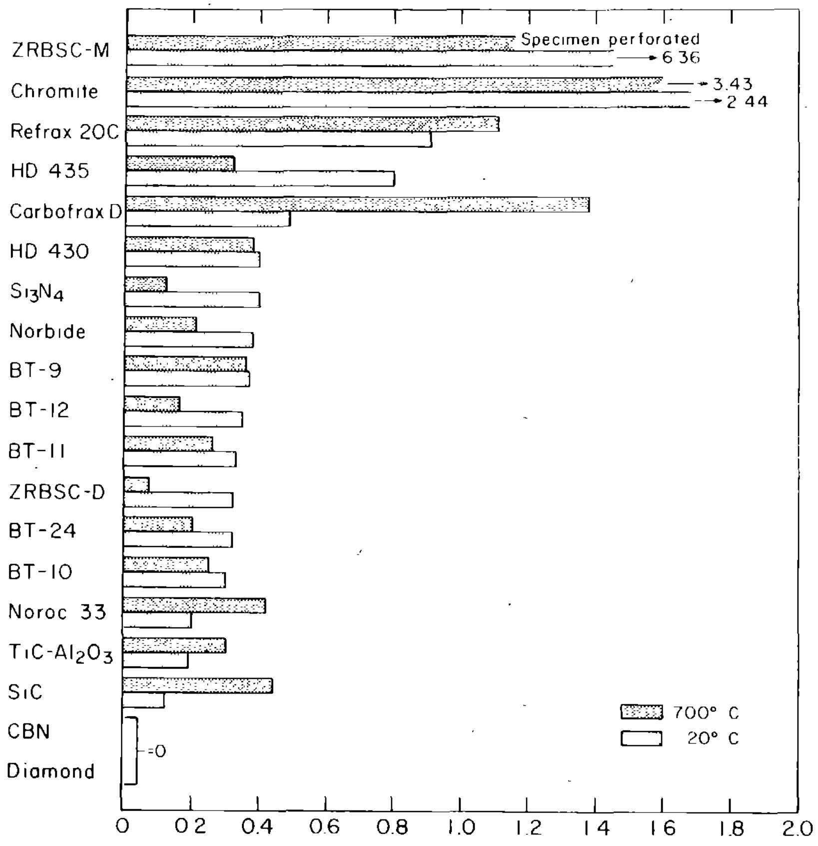

FIGURE 9. - REF's of commercially available ceramics (90° impingement).

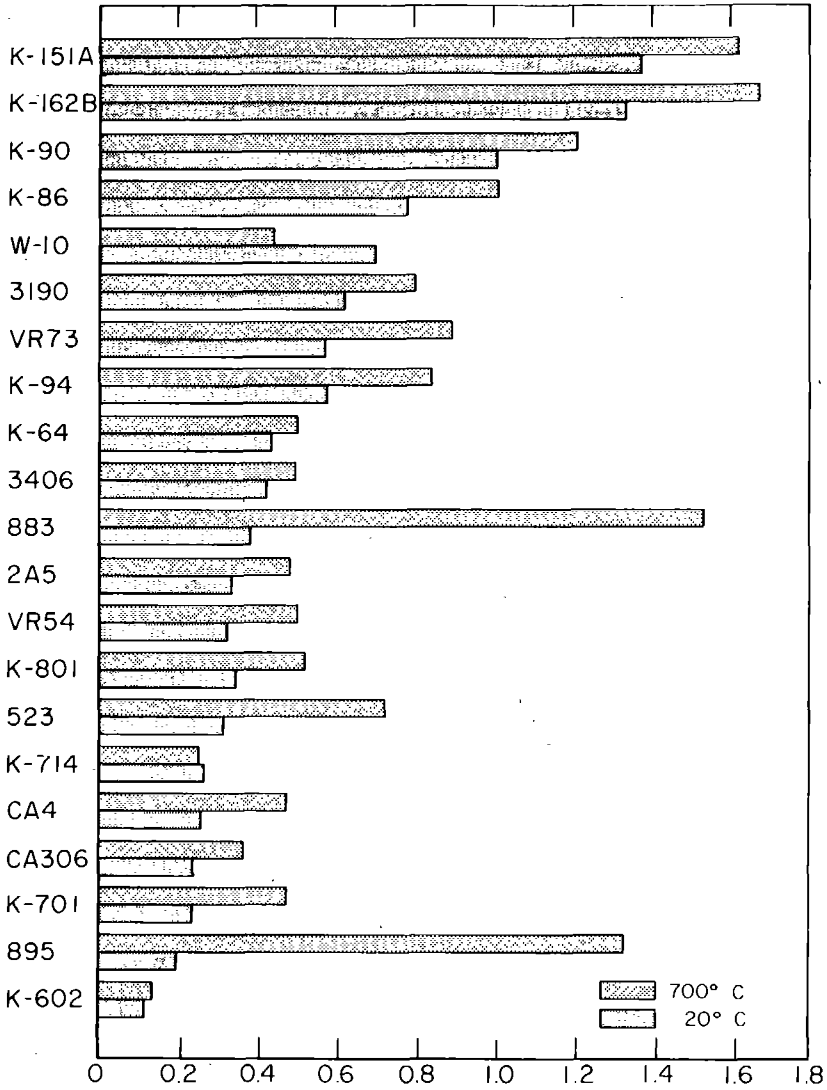

FIGURE 10. - REF's of commercially available cemented carbides (90° impingement).

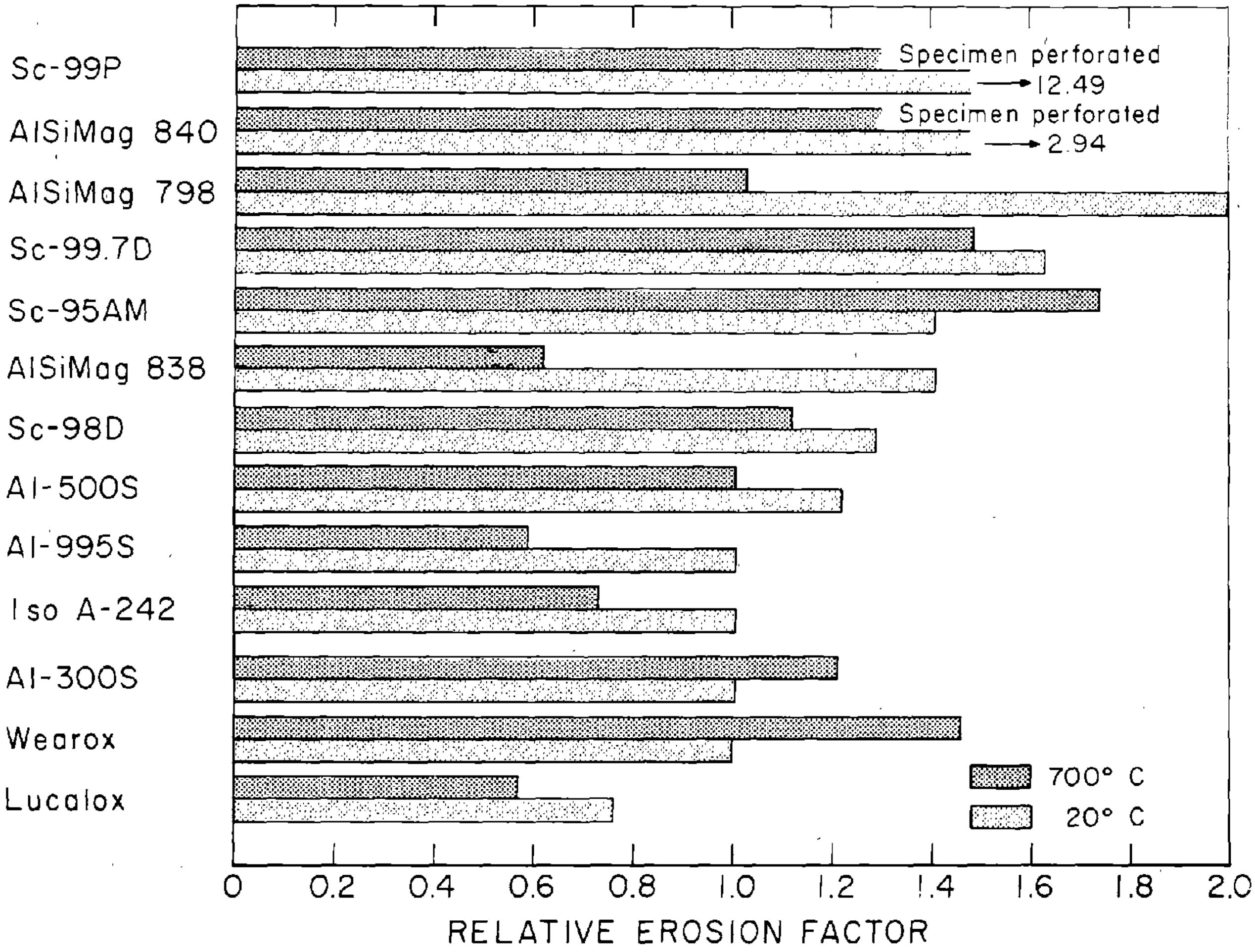

FIGURE 11. - REF's of commercially available sintered alumina ceramics (90° impingement).

In contrast with metallic materials, numerous cermets and ceramics, as illustrated in figures 9 and 10, had REF values that were over twice that of Stellite 6B at both room and elevated temperatures. Notable among these were a series of mixed ceramics that were prepared by pressing and sintering; several commercially available hot-pressed ceramics such as boron carbide (B_4C), silicon carbide (SiC), silicon nitride (Si_3N_4), cubic boron nitride (CBN), and synthetic diamond; and several tungsten carbides (WC).

Several ceramic coatings also had outstanding REF values. Data for coatings are listed in appendix B, tables B-4 through B-6. (Unlike single-composition materials, an REF value could not be accurately computed for all coated samples or samples with a protective layer. Instead, one of three conditions was noted--the sample was easily penetrated, penetration was retarded over a similar unprotected sample, or the sample was not penetrated.)

The outstanding coating materials included electrodeposited TiB_2, chemical vapor deposited (CVD) SiC, and boron diffused into Mo and Wc. Diffused

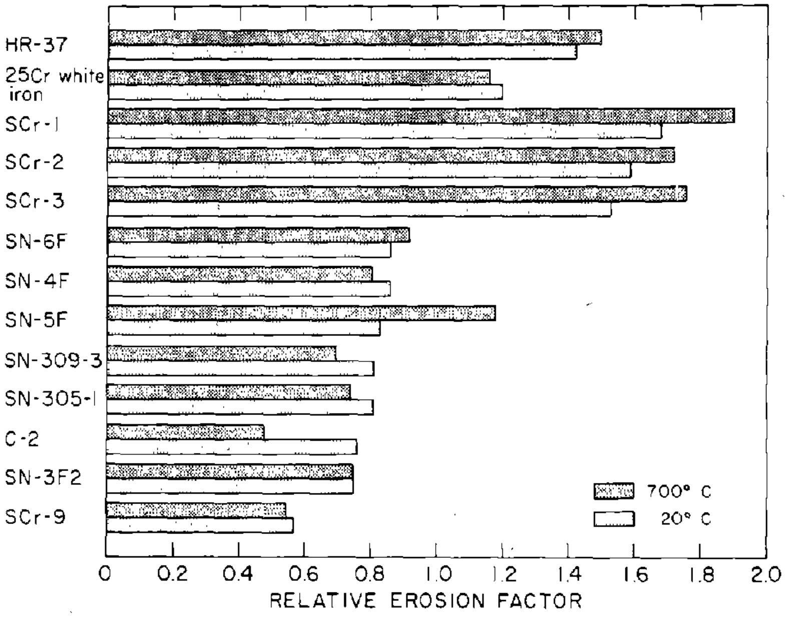

FIGURE 12. - REF's of Oregon Graduate Center carbonitrides and cast alloys (90° impingement).

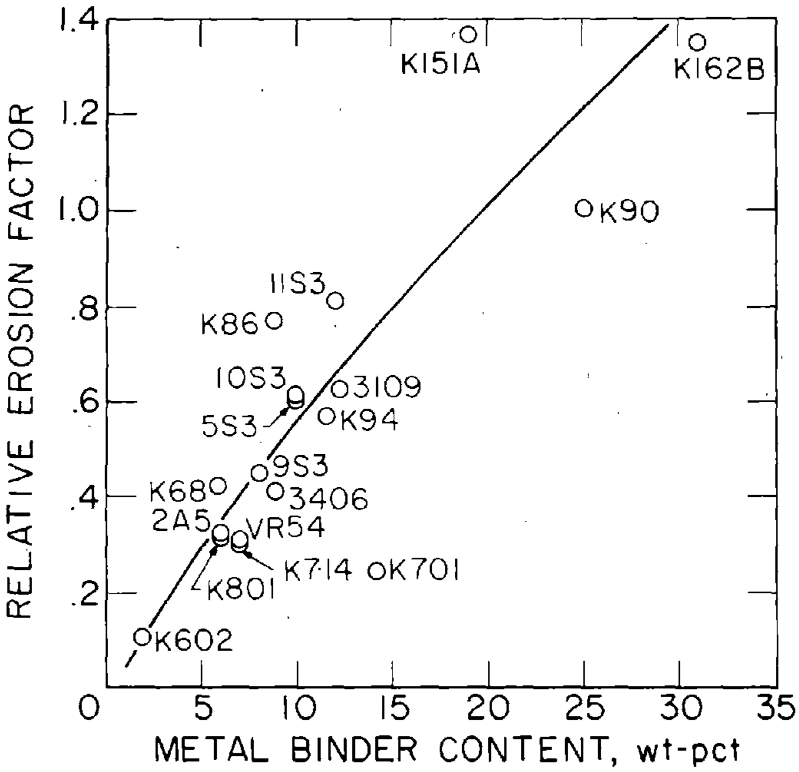

FIGURE 13. - Relative wear resistance of cemented carbides as a function of metal binder content.

boron improved the erosion resistance of WC and Mo at room temperature and a 90° impingement by more than 80 pct; at a 20° impingement, the improvement was more than fivefold. Electrodeposited TiB_2 was also exceptional and completely resisted erosion even after the test duration was extended to 10 minutes.

The thermal expansion of many coatings did not match that of the substrates. The result was that the coatings cracked in one or two heating and cooling cycles. The cracks exposed substrate material that was easily eroded, and the coatings were undermined. The TiB_2 and diffused boron coatings were noteworthy exceptions. Additionally, several coatings were inadequate when thin but were entirely protective when the thickness was increased to 50 to 75 um (2 to 3 mils).

No easily measured physical or mechanical property was found that could be used as a universal indicator of erosion resistance for either ceramic or metallic materials. There were, however, generalized correlations between erosion and binder content in carbides and porosity in pressed materials. In plotting the binder contents of various carbides against relative wear as shown in figure 13, a general trend was evident. With a decrease in binder content, erosion resistance was increased. The relationship suggested that the less resistant binder was eroded preferentially to the carbide phase. This mechanism was more apparent in several tests (not shown) on refractories in which the cement binders were eroded but the hard ceramic particles were not eroded.

The effect of porosity was demonstrated by several alumina ceramics. Lucalox, which is essentially 100 pct theoretically dense, was more than 1.5 times more erosion resistant than 95- to 98-pct-dense sintered aluminas. At an extreme, Lucalox had more than 10 times the erosion resistance of 99P, a porous alumina that was less than 70 pct of theoretical density. Similarly, hot-pressed Si_3N_4 had more than 10 times the erosion resistance of reaction-bonded (and less dense) Si_3N_4.

CONCLUSIONS

A data bank of erosion information on various materials has been prepared that can serve as a guide for the selection and application of erosion-resistant materials for coal gasifier valves. However, the variability of service conditions in any coal gasifier plant precluded general recommendations. Test procedures and equipment used in this investigation were designed to approximately simulate the erosion exposure of many valves. In addition to the erosion data presented, such additional factors as the possibility of corrosion, oxidation, and thermal expansion incompatibility must be considered.

Metallic alloys, other than tungsten and molybdenum, were shown to be at most no more than 30 pct more erosion resistant than Stellite 6B, which was used as a standard. Unfortunately, evidence from coal gasifier valve erosion failures indicates that even a twofold increase in erosion resistance over Stellite 6B is not adequate.

Certain ceramics and cermets were shown to be highly erosion resistant. Materials that had more than a fivefold increase in erosion resistance over metallic alloys included tungsten carbides with low binder contents, SiC, B_4C, Si_3N_4, and several other ceramics. All were fabricated to nearly theoretical density. Several adherent ceramic coatings or surface treatments were shown to have erosion resistance equal to that of solid ceramics. These classes of materials should develop the greatest acceptance as gasifier valve materials.

REFERENCES

1. Bitter, J. G. A. A Study of Erosion Phenomena, Parts 1 and 2. Wear, v. 6, 1963, pp. 5-169.

2. Bituminous Coal Research, Inc. Gas Generator Research and Development--Survey and Evaluation. Report L-156 to the Office of Coal Research, U.S. Dept. of the Interior, Washington, D.C., 1965, 650 pp.

3. Finnie, I. Erosion of Surfaces by Solid Particles. Wear, v. 3, 1960, pp. 87-103.

4. _____. The Mechanism of Erosion of Ductile Materials. Proc. 3d Material Cong. of Applied Mechanics, ASME, New York, 1958. Pergamon Press, London, 1978, pp. 527-532.

5. _____. Some Observations on the Erosion of Ductile Metals. Wear, v. 19, 1972, pp. 81-90.

6. Finnie, I., Y. Kabil, and J. Wolak. Erosion of Metals by Solid Particles. J. Materials, v. 2, No. 3, September 1967, pp. 682-700.

7. Forney, A. J., S. J. Gasior, W. P. Haynes, and S. Katell. A Process To Make High-Btu Gas From Coal. BuMines TPR 24, 1970, 6 pp.

8. Head, W. J., and M. E. Harr. The Development of a Model To Predict the Erosion of Materials by Natural Contaminants. Wear, v. 15, 1970, pp. 1-46.

9. Jennings, W. H., C. R. Manning, Jr., and W. J. Head. A Mechanistic Model for Prediction of Ductile Erosion. USAAMRDL-75-30, July 1975, 67 pp.

10. Lewis, P. S., A. J. Liberatore, and J. P. McGee. Strongly Caking Coal Gasified in a Stirred-Bed Producer. BuMines RI 7644, 1972, 11 pp.

11. Neilson, J. H., and A. Gilchrist. Erosion by a Stream of Solid Particles. Wear, v. 11, No. 2, 1968, pp. 111-122.

12. Oppelt, W. H., T. W. Kamps, C. H. Gronhovd, W. R. Kube, and R. McMurtie. Production of Crude Ammonia-Synthesis Gas From North Dakota Lignite in an Annular Retort Gasifier. BuMines RI 5297, 1957, 29 pp.

13. Ruff, A. W., and L. K. Ives. Measurement of Solid Particle Velocity in Erosive Wear. Wear, v. 35, 1975, pp. 195-199.

14. Sheldon, G. Erosion of Brittle Materials. Ph.D. Thesis, Univ. of Calif., Berkeley, Calif., 1965, 233 pp.

15. Sheldon, G. L., and I. Finnie. On the Ductile Behavior of Nominally Brittle Materials During Erosive Cutting. J. Eng. for Industry, v. 88, November 1966, pp. 387-392.

16. _____. The Mechanism of Material Removal in the Erosive Cutting of Brittle Materials. Trans. ASME, v. 88B, 1966, pp. 387-392.

17. Smeltzer, C. E., M. E. Gulden, and W. A. Compton. Mechanisms of Metal Removal by Impacting Dust Particles. J. Basic Eng., v. 92, 1970, pp. 639-654.

18. Wood, C. D., and P. W. Espenshade. Mechanisms of Dust Erosion. SAE Trans., v. 73, August 1965, pp. 515-523.

19. Young, J. P., and A. W. Ruff. Particle Erosion Measurements on Metals. J. Eng. Materials and Technology, v. 99, No. 2, April 1977, pp. 121-125.

APPENDIX A.--REVIEW OF EROSION VARIABLES

Knowledge of the variables affecting erosion is necessary to predict the severity of material loss when the conditions of a set of data do not precisely duplicate an actual field situation. Variables are described below.

1. Impingement angle--Erosion varies in a complex manner with impingement angle, the angle at which a particle strikes a surface. The relationship is illustrated in figure A-1 (6).[1] For ductile materials, the angle of maximum erosion is about 20°, although in a study by Smeltzer (17) using 5-μm alumina abrasive at 152 m/sec (500 ft/sec), the maximum occurred between 30° and 37.5° depending upon the target material. In a determination by Head (8) using rounded glass beads, the maximum occurred at 45°.

For brittle, ceramiclike materials, the angle of maximum erosion is 90°, but Sheldon (15) found that under certain conditions, the erosion rate-impingement angle relationship for a brittle material will approximate that of a ductile material. Sheldon changed the brittle erosion rate-impingement angle relationship when he reduced the size of the bombarding particles. He produced maxima at increasingly lower angles until finally, with 1,000-mesh particles, brittle behavior became indistinguishable from ductile behavior.

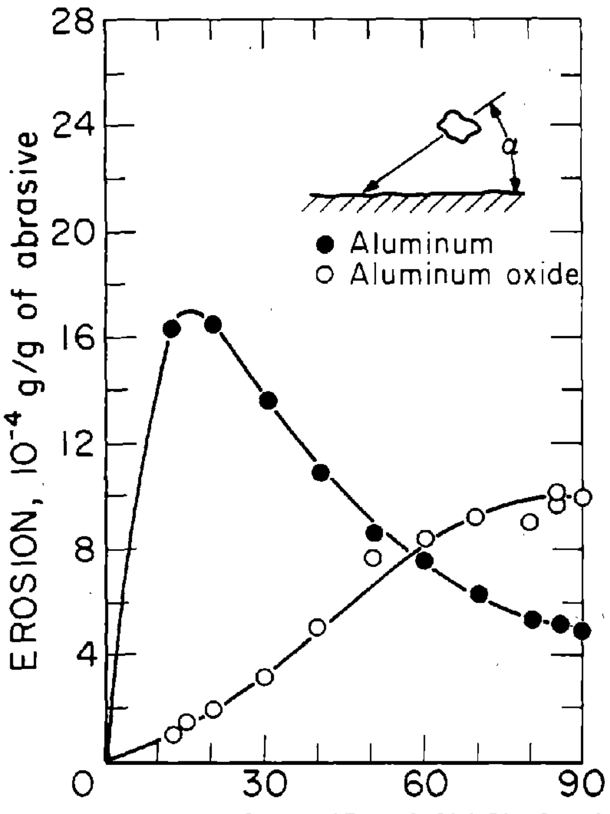

FIGURE A-1. - Weight removed by erosion as a function of angle of impingement for 1100-0 aluminum and high-density aluminum oxide (6). Both materials were eroded by 100-μm SiC particles at 152 m/sec.

The correct labeling of a material as either ductile or brittle is necessary. A hardened steel, for instance, that is normally thought to behave in a brittle manner in terms of impact resistance may behave in a ductile manner in terms of erosion. Additionally, data given for only one angle may give a false impression of the total erosion resistance of a material.

2. Particle velocity--Through its motion, a particle has a quantity of kinetic energy that is available to do damage to a material upon impact. Both the kinetic energy and the damage increase with an increase in particle velocity. The damage is equatable to a power function exponent of the

---

[1] Underlined numbers in parentheses refer to items in the list of references preceding the appendixes.

velocity which is within a range of 2.1 to 2.4 for ductile materials (6). For brittle materials the power function exponent may be as high as 4.4 (14).

3. Particle flux--In general, an increase in the quantity of abrasive impinging upon a surface produces a proportional increase in erosion. At high concentrations, erosion efficiency decreases, presumably because the particles expend their energy in hitting each other rather than in removing material from a surface. At low concentrations, Wood (18), Smeltzer (17), and Young (19) all reported greater erosion efficiency per particle.

4. Particle size--Within limits, erosion is directly related to particle size. However, there is disagreement as to where the maxima develop with increasing particle size. Finnie (5), for example, found that size had no effect above 100 μm, while Head (8) found that the erosion of carbides increased with particle size up to 300 μm, and thereafter decreased up to 900 μm. Sheldon (16) noted no size effect on aluminum for 51-, 125-, and 250-μm particles, but for smaller particles, he reported decreased erosion.

5. Particle shape--Sharp particles produce greater erosion in ductile materials than do rounded particles.

6. Particle hardness--Particle hardness will not influence the erosion of ductile materials provided the eroding particles are harder than the material undergoing erosion.

7. Time--Time has a linear effect on erosion rates unless the actual impingement angle is sufficiently altered by the developing crater, in which case erosion may increase or decrease accordingly.

8. Temperature--The effect of temperature is not well known. A partial explanation of the effect is included within the text.

9. Material factors--There are no reliable material properties that universally correlate with erosion resistance. For certain pure materials, Finnie (6) found that erosion is proportional to Vickers hardness, but the same researchers also found that erosion is constant for different hardnesses of the same steel. Similarly, Smeltzer (17) noted that differing heat treatments on 2024 aluminum, 17-7 PH stainless steel, 410 stainless steel, and Ti-6Al-4V alloys had no effect. Finnie (4) suggested flow stress as a universal indicator of ductile erosion resistance, but his equations require the use of difficult-to-measure micro flow stress values that are considerably greater than the easily measured macro flow stress values obtainable from a tensile test. In addition, melting point and elastic modulus have been shown to have a rough correlation with erosion (8, 17).

APPENDIX B.--EROSION TEST DATA

TABLE B-1. - Room-temperature erosion test results--90° impingement, 27-μm Al_2O_3 particles, 5-g/min particle flow, 170-m/sec particle velocity, 3-min test duration, N_2 atmosphere

Test material	Fabrication method[1]	Composition	Source[1]	Relative erosion factor[2]
SC-99P	ps	99+ Al_2O_3	Krohn	12.49
ZRBSC-M	hp	ZrB_2-SiC-graphite	N	6.36
CbC	c	Not applicable	Unknown	3.56
HfC	c	Not applicable	Unknown	3.49
5527	hp	45$MgAl_2O_4$-55MgO	NBS	3.39
AlSiMag 840	ps	Modified Al_2O_3	3M	2.94
4310	hp	97$MgAl_2O_4$-3MgO	NBS	2.56
TaC	c	Not applicable	Unknown	2.48
4879	hp	91$MgAl_2O_4$-9MgO	NBS	2.44
Chromite	ps	Unknown	UCAR	2.44
AD-995	ps	99.5Al_2O_3	Coors	2.25
AlSiMag 798	ps	85Al_2O_3	3M	2.00
$MgAl_2O_4$	hp	Not applicable	NBS	1.84
SCr-1	ps	85.5(Ti,Cr)CN-14.5Ni	OGC	1.67
SC-99.7D	ps	99.7Al_2O_3	Krohn	1.63
SCr-2	ps	85.8(Ti,Cr)CN-14.2Ni	OGC	1.58
SCr-3	ps	86(Ti,Cr)CN-14Ni	OGC	1.52
SC-95AM	ps	94Al_2O_3	Krohn	1.41
AlSiMag 838	ps	99.5Al_2O_3	3M	1.41
HR-37	c	5Cr-1Ti-14W-8V-3.9C-13Mn-bal Fe	OGC	1.41
K151A	ps	19Ni binder	K	1.37
K162B	ps	25Ni + 6Mo binder	K	1.35
SC-98D	ps	98Al_2O_3	Krohn	1.29
Ti-6Al-4V	c	Not applicable	Unknown	1.26
Haynes 93	c	17Cr-16Mo-6.3Co-3C-bal Fe	Stel	1.25
Al-500S	ps	94Al_2O_3	Wesgo	1.22
Graph-Air	w	1.4C-1.9Mn-1.2Si-1.9Ni-1.5Mo-bal Fe	TRB	1.19
25Cr iron	c	25Cr-2Ni-2Mn-0.5Si-3.5C-bal Fe	OGC	1.19
AZ-27Cr	ps	TiC in D_2 die steel	OGC	1.14
AZ-31HF	ps	TiC in H-13 die steel	OGC	1.14
FeTiC-23	ps	TiC-(Fe,Ni,Cr,Mo)C	OGC	1.14
FeTiC-29HS10	ps	TiC in M-10 die steel	OGC	1.12
AZ-20-1	ps	TiC-(Fe,Ni,Cr,Mo)C	OGC	1.11
AZ-30HS42	ps	TiC in M-42 steel	OGC	1.10
Stellite 6K	w	30Cr-4.5W-1.5Mo-1.7Cr-bal Co	Stel	1.08
Al-995S	ps	99.5Al_2O_3	Wesgo	1.08
Iso A-242	ps	Al_2O_3	Green	1.07
Al-300S	ps	97.6Al_2O_3	Wesgo	1.04
Stellite 3	c	31Cr-12.5W-2.4C-bal Co	Stel	1.04
K90	ps	25 binder	K	1.01
Stellite 6B	w	30Cr-4.5W-1.5Mo-1.2C-bal Co	Stel	1.00
304 SS	w	17Cr-9Ni-2Mn-1Si-bal Fe	Unknown	1.00
Wearox	ps	99.5Al_2O_3	Wesgo	1.00
316 SS	w	17Cr-12Ni-2Mn-1Si-2.5Mo-bal Fe	Unknown	.99
Haynes 188	w	22Cr-14.5W-22Ni-0.15C-bal Co	Stel	.97
Haynes 25	w	20Cr-15W-10Ni-1.5Mn-0.15C-bal Co	Stel	.96
430 SS	w	17Cr-1Mn-1Si-0.1C-bal Fe	Unknown	.93
MoTiCN	ps	Not applicable	TWCA	.93
HK-40	c	26Cr-20Ni-0.4C-bal Fe	Unknown	.93
Inconel 600	w	76Ni-15.5Cr-8Fe	HA	.92
RA 330	w	19Cr-35Ni-1.5Mn-1.3Si-bal Fe	RA	.91
Refrax 20C	ps	SiC-Si_3N_4 bond	Carbor	.91
Incoloy 800H	w	32.5Ni-21Cr-0.07C-46Fe	HA	.91
Beta III Ti	w	11.5Mo-6Zr-4.5Sn-bal Ti	Unknown	.90
SN-6F	ps	85(Ti,Mo)CN-12Ni-3Mo	OGC	.85

See footnotes at end of table.

TABLE B-1. - Room-temperature erosion test results--90° impingement, 27-μm Al_2O_3 particles, 5-g/min particle flow, 170-m/sec particle velocity, 3-min test duration, N_2 atmosphere--Continued

Test material	Fabrication method[1]	Composition	Source[1]	Relative erosion factor[2]
SN-4F	ps	84(Ti,Mo)CN-13Ni-3Mo	OGC	0.85
Incoloy 800	w	32.5Ni-46Fe-21Cr	HA	.83
SN-5F	ps	85(Ti,Mo)CN-12Ni-3Mo	OGC	.82
11S-3	ps	85(Ti,Mo)CN-12Ni-3Mo	OGC	.82
SN-305-1	ps	94(Ti,Mo)CN-5Ni-1Mo	OGC	.80
SN-309-3	ps	89(Ti,Mo)CN-9Ni-2Mo	OGC	.80
HD 435	NAp	Recrystallized SiC	N	.80
RA-333	w	25Cr-1.5Mn-1.3Si-3Co-3Mo-3W-18Fe-bal Ni	RA	.80
MoTiCN	c	Not applicable	TWCA	.80
K86	ps	8.8 binder	K	.78
Inconel 671	w	50Ni-48Cr-0.4Ti	HA	.77
Lucalox	NAp	Densified Al_2O_3	GE	.76
Mild steel	w	0.15C-bal Fe	Unknown	.76
C-2	ps	97(Ti,Mo)CN-2Ni-0.5Mo	OGC	.75
SN-3F2	ps	84(Ti,Mo)CN-13Ni-3Mo	OGC	.74
FeWC-33	ps	Not applicable	OGC	.73
W-10	ps	90W-10(Ni,Cu,Fe)	K	.70
3109	ps	12.2 binder	K	.62
10S-3	ps	90(W,Cr)C-10Ni	OGC	.62
5S-3	ps	90WC-5Co-5Ni	OGC	.61
K94	ps	11.5 binder	K	.57
VR73	ps	71WC-12TiC-10TaC,CbC-6.5Co binder	F	.57
SCr-9	ps	84(Ti,Cr,Mo)CN-3Mo-13Ni	OGC	.56
Mo	w	Not applicable	Unknown	.52
Carbofrax D	ps	SiC-ceramic bond	Carbor	.49
W	w	Not applicable	GE	.48
9S-3	ps	92(W,Cr)C-8Ni	OGC	.46
K68	ps	5.8 binder	K	.43
3406	ps	7.8 binder	K	.42
HD 430	NAp	Recrystallized SiC	N	.40
Si_3N_4	hp	Not applicable	N	.40
Norbide	hp	B_4C	N	.38
883	ps	WC-6Co binder	Carb	.38
BT-9	ps	$2MgO-25TiB_2-3.5WC-bal\ Al_2O_3$	OGC	.37
BT-12	ps	$1.5MgO-49TiB_2-3.5WC-bal\ Al_2O_3$	OGC	.35
2A5	ps	WC-6Co binder	F	.33
BT-11	ps	$1.7MgO-38TiB_2-3.5WC-bal\ Al_2O_3$	OGC	.33
ZRBSC-D	hp	ZrB_2-SiC	N	.32
VR54	ps	WC-7Co binder	F	.32
BT-24	ps	$2MgO-30TiB_2-3.5WC-bal\ Al_2O_3$	OGC	.32
K801	ps	6Ni binder	K	.32
523	ps	WC-TiC coating	Carb	.31
BT-10	ps	$2MgO-30TiB_2-3.5WC-bal\ Al_2O_3$	OGC	.30
K714	ps	6Co + 1Cr binder	K	.26
K701	ps	10.2Co + 4Cr binder	K	.25
CA 4	ps	WC-6Co binder	Carmet	.25
CA 306	ps	WC-6Co binder	Carmet	.23
Noroc-33	hp	Si_3N_4-SiC	N	.20
TiC-Al_2O_3	ps	Not applicable	B and W	.19
895	ps	WC-6Co binder	Carb	.19
SiC	hp	Not applicable	N	.12
K602	ps	<1.5 binder	K	.11
SiC	NAp	98 pct dense	GE	.05
CBN	NAp	Not applicable	GE	0
GE diamond	NAp	Not applicable	GE	0

[1] Abbreviations are explained in table B-7.

[2] REF (relative erosion factor) = $\frac{\text{vol. loss material}}{\text{vol. loss Stellite 6B}}$.

TABLE B-2. - Room-temperature erosion test results--20° impingement, 27-μm Al_2O_3 particles, 5-g/min particle flow, 170-m/sec particle velocity, 3-min test duration, N_2 atmosphere

Test material	Fabrication method[1]	Composition	Source[1]	Relative erosion factor[2]
SC-99P	ps	99+ Al_2O_3	Krohn	16.42
Ti-6Al-4V	w	Not applicable	Unknown	1.56
Mild steel	w	0.15C-bal Fe	Unknown	1.19
316 SS	w	17Cr-12Ni-2Mn-1Si-2.5Mo-bal Fe	Unknown	1.19
Graph-Air	w	1.4C-1.9Mn-1.2Si-1.9Ni-1.5Mo-bal Fe	TRB	1.16
Incoloy 800	w	32.5Ni-46Fe-21Cr	HA	1.08
Incoloy 800H	w	32.5Ni-21Cr-0.07C-46Fe	HA	1.08
Inconel 671	w	50Ni-48Cr-0.4Ti	HA	1.06
HK-40	c	26Cr-20Ni-0.4C-bal Fe	Unknown	1.04
RA 330	w	19Cr-35Ni-1.5Mn-1.3Si-bal Fe	RA	1.04
RA 333	w	25Cr-1.5Mn-1.3Si-3Co-3Mo-18Fe-bal Ni	RA	1.04
Stellite 6B	w	30Cr-4.5W-1.5Mo-1.2C-bal Co	Stel	1.00
AlSiMag 840	ps	Modified Al_2O_3	3M	.86
AlSiMag 798	ps	85Al_2O_3	3M	.64
Mo	w	Not applicable	Unknown	.52
W-10	ps	90W-10(Ni,Cu,Fe)	K	.48
SC-99.7D	ps	99.7Al_2O_3	Krohn	.39
W	w	Not applicable	GE	.37
SC-98D	ps	98Al_2O_3	Krohn	.30
SC-95AM	ps	94Al_2O_3	Krohn	.29
Refrax 20C	ps	SiC-Si_3N_4 bond	Carbor	.27
AlSiMag 614	ps	96Al_2O_3	3M	.26
AlSiMag 838	ps	99.5Al_2O_3	3M	.25
Al-995S	ps	99.5Al_2O_3	Wesgo	.22
Wearox	ps	99.5Al_2O_3	Wesgo	.20
Norbide	hp	B_4C	N	.16
ZRBSC-D	hp	ZrB_2-SiC	N	.14
Al-500S	ps	94Al_2O_3	Wesgo	.11
Al-300S	ps	97.6Al_2O_3	Wesgo	.09
Noroc 33	hp	Si_3N_4-SiC	N	.05
BT-11	ps	1.7MgO-38TiB -3.5WC-bal Al_2O_3	OGC	.05
Carbofrax D	ps	SiC-ceramic bond	Carbor	.05
SiC	hp	Not applicable	N	.05
Si_3N_4	hp	Not applicable	N	.04
Lucalox	NAp	Densified Al_2O_3	GE	.03
K701	ps	10.2Co + 4Cr binder	K	.02
K714	ps	6Co + 1Cr binder	K	.01
K602	ps	<1.5 binder	K	.01

[1] Abbreviations are explained in table B-7.

[2] REF (relative erosion factor) = $\frac{\text{vol. loss material}}{\text{vol. loss Stellite 6B}}$.

TABLE B-3. - 700° C erosion test results--90° impingement, 27-μm Al_2O_3 particles, 5-g/min particle flow, 170-m/sec particle velocity, 3-min test duration, N_2 atmosphere

Test material	Fabrication method[1]	Composition	Source[1]	Relative erosion factor[2]
ZRBSC-M	hp	ZrB_2-SiC-graphite	N	High
AlSiMag 840	ps	Modified Al_2O_3	3M	High
SC-99P	ps	99+ Al_2O_3	Krohn	High
Chromite	ps	Not applicable	UCAR	3.43
5527	hp	$45MgAl_2O_4$-55MgO	NBS	2.84
4879	hp	$91MgAl_2O_4$-9MgO	NBS	2.77
4310	hp	$97MgAl_2O_4$-3MgO	NBS	2.76
$MgAl_2O_4$	hp	Not applicable	NBS	2.56
SCr-1	ps	85.5(Ti,Cr)CN-14.5Ni	OGC	1.89
SCr-3	ps	86(Ti,Cr)CN-14Ni	OGC	1.75
SC-95AM	ps	$94Al_2O_3$	Krohn	1.74
SCr-2	ps	85.8(Ti,Cr)CN-14.2Ni	OGC	1.71
K162B	ps	25Ni + 6Mo binder	K	1.67
K151A	ps	19Ni binder	K	1.62
Stellite 3	c	31Cr-12.5W-2.4C-bal Co	Stel	1.61
883	ps	WC-6Co binder	Carb	1.53
SC-99.7D	ps	$99.7Al_2O_3$	Krohn	1.49
HR-37	c	5Cr-1Ti-14W-8V-3.9C-13Mn-bal Fe	OGC	1.49
Wearox	ps	$99.5Al_2O_3$	Wesgo	1.46
Carbofrax D	ps	SiC-ceramic bond	Carbor	1.38
895	ps	WC-6Co binder	Carb	1.32
Mo	w	Not applicable	Unknown	1.32
K90	ps	25 binder	K	1.21
Al-300S	ps	$97.6Al_2O_3$	Wesgo	1.21
SN-5F	ps	85(Ti,Mo)CN-12Ni-3Mo	OGC	1.17
25 Cr iron	c	25Cr-2Ni-2Mn-0.5Si-3.5C-bal Fe	OGC	1.16
AlSiMag 798	ps	$85Al_2O_3$	3M	1.15
Refrax 20C	ps	SiC-Si_3N_4 bond	Carbor	1.15
SC-98D	ps	$98Al_2O_3$	Krohn	1.12
Stellite 6K	w	30Cr-4.5W-1.5Mo-1.7C-bal Co	Stel	1.06
Al-500S	ps	$94Al_2O_3$	Wesgo	1.04
K86	ps	8.8Co binder	K	1.03
Stellite 6B	w	30Cr-4.5W-1.5Mo-1.2C-bal Co	Stel	1.00
Haynes 93	c	17Cr-16Mo-6.3Co-3C-bal Fe	Stel	1.00
11S-3	ps	88(W,Cr)C-10Ni	OGC	.99
TiCN	ps	Not applicable	TWCA	.98
10S-3	ps	90(W,Cr)C-10Ni	OGC	.92
SN-6F	ps	85(Ti,Mo)CN-12Ni-3Mo	OGC	.91
VR73	ps	71WC-12TiC-10TaC-CbC-6.5Co	F	.89
AlSiMag 614	ps	$96Al_2O_3$	3M	.87
5S-3	ps	90WC-5Co-5Ni	OGC	.87
9S-3	ps	92(W,Cr)C-8Ni	OGC	.86
Haynes 25	w	20Cr-15W-10Ni-0.15C-bal Co	Stel	.85
K94	ps	11.5 binder	K	.84
Haynes 188	w	22Cr-14.5W-22Ni-0.15C-bal Co	Stel	.83
RA-333	w	25Cr-1.5Mn-1.3Si-3Co-3Mo-3W-18Fe-bal Ni	RA	.80
SN-4F	ps	84(Ti,Mo)CN-13Ni-3Mo	OGC	.80
3109	ps	12.2 binder	K	.80
RA-330	w	19Cr-35Ni-1.5Mn-1.3Si-bal Fe	RA	.79

See footnotes at end of table.

TABLE B-3. - 700° C erosion test results--90° impingement, 27-μm Al_2O_3 particles, 5-g/min particle flow, 170-m/sec particle velocity, 3-min test duration, N_2 atmosphere--Continued

Test material	Fabrication method[1]	Composition	Source[1]	Relative erosion factor[2]
HK-40	c	26Cr-20Ni-0.4C-bal Fe	Unknown	0.78
SN-3F2	w	83(Ti,Mo)CN-13Ni-3Mo	OGC	.74
304 SS	w	17Cr-9Ni-2Mn-1Si-bal Fe	Unknown	.73
Iso A-242	ps	Not applicable	Green	.73
SN-305-1	ps	94(Ti,Mo)CN-5Ni-1Mo	OGC	.73
523	ps	WC-TiC coating	Carb	.72
SN-309-3	ps	89(Ti,Mo)CN-9Ni-2Mo	OGC	.69
AlSiMag 838	ps	99.5Al_2O_3	3M	.62
Inconel 671	w	50Ni-48Cr-0.4Ti	HA	.62
430 SS	w	17Cr-1Mn-1Si-0.1C-bal Fe	Unknown	.62
Inconel 600	w	76Ni-15.5Cr-8Fe	HA	.61
Al-995S	ps	99.5Al_2O_3	Wesgo	.59
Lucalox	NAp	Densified Al_2O_3	GE	.57
Beta III Ti	w	11.5Mo-6Zr-4.5Sn-bal Ti	Unknown	.57
Incoloy 800	w	32.5Ni-21Cr-46Fe	HA	.57
316 SS	w	17Cr-12Ni-2Mn-1Si-2.5Mo-bal Fe	Unknown	.56
Ti-6Al-4V	w	Not applicable	Unknown	.54
Incoloy 800H	w	32.5Ni-21Cr-0.07C-46Fe	HA	.54
SCr-9	ps	84(Ti,Cr,Mo)CN-3Mo-13Ni	OGC	.54
K68	ps	5.8 binder	K	.50
VR-54	ps	WC-7Co binder	F	.50
3406	ps	7.8 binder	K	.49
2A5	ps	WC-6Co binder	F	.48
K701	ps	10.2Co + 4Cr binder	K	.47
CA 4	ps	WC-6Co binder	Carmet	.47
C-2	ps	97(Ti,Mo)CN-2Ni-0.5Mo	OGC	.47
K801	ps	6Ni binder	K	.46
SiC	hp	Not applicable	N	.44
W-10	ps	90W-10(Ni,Cu,Fe)	K	.44
Noroc 33	hp	Si_3N_4-SiC	N	.42
HD 430	NAp	Recrystallized SiC	N	.38
CA 306	ps	WC-6Co binder	Carmet	.36
BT-9	ps	2MgO-25TiB_2-3.5WC-bal Al_2O_3	OGC	.36
HD 435	NAp	Recrystallized SiC	N	.32
TiC-Al_2O_3	ps	Not applicable	B and W	.30
BT-11	ps	1.7MgO-38TiB_2-3.5WC-bal Al_2O_3	OGC	.26
K714	ps	6Co + 1Cr binder	K	.25
BT-10	ps	2MgO-30TiB_2-3.5WC-bal Al_2O_3	OGC	.25
Norbide	hp	B_4C	N	.21
BT-24	ps	2MgO-30TiB_2-3.5WC-bal Al_2O_3	OGC	.20
W	w	Not applicable	GE	.17
BT-12	ps	1.5MgO-49TiB_2-3.5WC-bal Al_2O_3	OGC	.16
K602	ps	<1.5 binder	K	.13
Si_3N_4	hp	Not applicable	N	.12
ZRBSC-D	NAp	ZrB_2-SiC	N	.07
SiC	NAp	98 pct dense	GE	.02
Diamond	NAp	Not applicable	GE	0
CBN	NAp	Not applicable	GE	0

[1] Abbreviations are explained in table B-7.

[2] REF (relative erosion factor) = $\frac{\text{vol. loss material}}{\text{vol. loss Stellite 6B}}$.

TABLE B-4. - Room-temperature erosion test results on coated materials--90° impingement, 27-μm Al_2O_3 particles, 5-g/min particle flow, 170-m/sec particle velocity, 3-min test duration, N_2 atmosphere

Test material	Fabrication method[1]	Composition	Source[1]	Relative erosion factor[2]
TiC	CVD	TiC on unknown substrate	Unknown	([3])
Al_2O_3	CVD	Al_2O_3 on unknown substrate	Unknown	([3])
TiCN	CVD	TiCN on unknown substrate	Unknown	([3])
TiN	CVD	TiN on unknown substrate	Unknown	([3])
TiCN	CVD	TiCN on Ti-6Al-4V	Unknown	([4])
TiCN	CVD	TiCN on Inconel 718	Unknown	([4])
TiCN	CVD	TiCN on WC	Unknown	([4])
Borofuse Stellite 31	pc	B on 25Cr-10.5Ni-2Fe-7.5W-0.5C-bal Co	Stel-MDC	1.40
Ni-Cr-B-Cu	Plasma	0.5C-4Si-16Cr-4B-4Fe-2.4Cu-2.4Mo-2.4W-bal Ni	CWS	1.32
Borofuse Stellite 6	pc	B on 28Cr-4W-1C-bal Co	Stel-MDC	1.29
Cr_2O_3	Plasma	Cr_2O_3-5SiO_2-3TiO_2	CWS	1.23
WC	Plasma	35(WC+8Ni)-11Cr-2.5B-2.5Fe-2.5Si-0.5C-bal Ni	CWS	1.11
Borofuse Stellite 3	pc	B on 31Cr-12.5W-2.4C-bal Co	Stel-MDC	.92
W	CVD	Pure coating	RMRC	.53
Borofuse MT-104	pc	B on 0.5Ti-0.08Zr-0.03C-bal Mo	Syl-MDC	.30
Borofuse PM moly	pc	B on Mo	CM-MDC	.25
SiC	CVD	SiC on C converted to SiC	Unknown	.06
SiC	CVD	Pure coating	Unknown	.05
Borofuse WC	pc	B on WC	MDC	.02
TiB_2	e	TiB_2 on Ni	CPMRC	0
18B-11	e	TiB_2 on 310 SS	UT	0
19A-13	e	TiB_2 on 310 SS	UT	0

[1] Abbreviations are explained in table B-7.

[2] REF (relative erosion factor) = $\frac{\text{vol. loss material}}{\text{vol. loss Stellite 6B}}$.

[3] Ready penetration--coating too thin.

[4] Retarded penetration--coating 0.002 in thick.

TABLE B-5. - Room-temperature erosion test results on coated materials--20° impingement, 27-μm Al_2O_3 particles, 5-g/min particle flow, 170-m/sec particle velocity, 3-min test duration, N_2 atmosphere

Test material	Fabrication method[1]	Composition	Source[1]	Relative erosion factor[2]
TiC	CVD	TiC on unknown substrate	Unknown	([3])
Al_2O_3	CVD	Al_2O_3 on unknown substrate	Unknown	([3])
TiCN	CVD	TiCN on unknown substrate	Unknown	([3])
TiN	CVD	TiN on unknown substrate	Unknown	([3])
TiCN	CVD	TiCN on Ti-6Al-4V	Unknown	0
TiCN	CVD	TiCN on Inconel 718	Unknown	0
TiCN	CVD	TiCN on WC	Unknown	([4])
Ni-Cr-B-Cu	Plasma	0.5C-4Si-16Cr-4B-4Fe-2.4Cu-2.4Mo-2.4W-bal Ni	CWS	0.98
WC	Plasma	35(WC+8Ni)-11Cr-2.5B-2.5Fe-2.5Si-0.5C-bal Ni	CWS	.72
Cr_2O_3	Plasma	Cr_2O_3-5SiO_2-3TiO_2	CWS	.61
Borofuse Stellite 6	pc	B on 28Cr-4W-1C-bal Co	Stel-MDC	.45
Borofuse Stellite 31	pc	B on 25Cr-10.5Ni-2Fe-7.5W-0.5C-bal Co	Stel-MDC	.40
Borofuse Stellite 3	pc	B on 31Cr-12.5W-2.4C-bal Co	Stel-MDC	.37
SiC	CVD	Pure coating	Unknown	.20
SiC	CVD	SiC on C converted to SiC	Unknown	.13
Borofuse PM moly	pc	B on Mo	CM-MDC	.09
Borofuse MT-104	pc	B on 0.5Ti-0.08Zr-0.03C-bal Mo	Syl-MDC	.03
Borofuse WC	pc	B on WC	MDC	.01
TiB_2	e	TiB_2 on Ni	CPMRC	0
18B-11	e	TiB_2 on 310 SS	UT	0
19A-13	e	TiB_2 on 310 SS	UT	0

[1] Abbreviations are explained in table B-7.

[2] REF (relative erosion factor) = $\dfrac{\text{vol. loss material}}{\text{vol. loss Stellite 6B}}$.

[3] Ready penetration--coating too thin.

[4] Retarded penetration--coating 0.002 in thick.

TABLE B-6. - 700° C erosion test results on coated materials--90° impingement, 27-μm Al_2O_3 particles, 5-g/min particle flow, 170-m/sec particle velocity, 3-min test duration, N_2 atmosphere

Test material	Fabrication method[1]	Composition	Source[1]	Relative erosion factor[2]
TiC	CVD	TiC on unknown substrate	Unknown	(3)
Al_2O_3	CVD	Al_2O_3 on unknown substrate	Unknown	(3)
TiCN	CVD	TiCN on unknown substrate	Unknown	(3)
TiN	CVD	TiN on unknown substrate	Unknown	(3)
Ni-Cr-B-Cu	Plasma	0.5C-4Si-16Cr-4B-4Fe-2.4Cu-2.4Mo-2.4W-bal Ni	CWS	2.79
WC	Plasma	35(WC-8Ni)-11Cr-2.5B-2.5F-2.5Si-0.5C-bal Ni.	CWS	2.06
Borofuse Stellite 6.	pc	B on 28Cr-4W-1C-bal Co	Stel-MDC	1.40
Borofuse Stellite 31	pc	B on 25Cr-10.5Ni-2Fe-7.5W-0.5C-bal Co	Stel-MDC	1.37
Borofuse Stellite 3.	pc	B on 31Cr-12.5W-2.4C-bal Co	Stel-MDC	.83
Borofuse WC	pc	B on WC	MDC	.72
Borofuse PM moly	pc	B on Mo	CM-MDC	.28
W	CVD	Pure coating	RMRC	.25
Borofuse MT-104	pc	B on 0.5Ti-0.08Zr-0.03Cr-bal Mo	Syl-MDC	.19
SiC	CVD	Pure coating	Unknown	0
SiC	CVD	SiC on C converted to SiC	Unknown	0
TiB_2	e	TiB_2 on Ni	CPMRC	0
18B-11	e	TiB_2 on 310 SS	UT	0
19A-13	e	TiB_2 on 310 SS	UT	0

[1] Abbreviations are explained in table B-7.

[2] REF (relative erosion factor) = $\dfrac{\text{vol. loss material}}{\text{vol. loss Stellite 6B}}$.

[3] Ready penetration--coating too thin.

TABLE B-7. - Abbreviations used in tables B-1 through B-6

3M	American Lava Corp., Subsidiary of Minnesota Mining & Manufacturing Co.
B and W	Babcox and Wilcox.
Carb	Carboloy Systems Dept., General Electric Co.
Carbor	Carborundum Co.
Carmet	Carmet Co., Allegheny Ludlum Steel Corp.
c	Cast.
CVD	Chemical vapor deposited.
CM	Climax Molybdenum Co.
CPMRC	College Park Metallurgy Research Center (now Avondale Metallurgy Research Center), Bureau of Mines.
Coors	Coors, USA.
CWS	CWS Corp.
e	Electrodeposited.
F	Fansteel, Inc.
GE	General Electric Co.
Green	A. P. Green
hp	Hot pressed.
HA	Huntington Alloy Products Div., International Nickel Co.
K	Kennametal, Inc.
Krohn	Krohn Ceramics Corp.
MDC	Materials Development Corp.
NBS	National Bureau of Standards.
N	Norton Co.
NAp	Not applicable.
OGC	Oregon Graduate Center.
pc	Pack cementation.
ps	Pressed and sintered.
RMRC	Rolla Metallurgy Research Center, Bureau of Mines.
RA	Rolled Alloys Corp.
Stel	Stellite Div., Cabot Corp.
Syl	Sylvania Electric Products Inc.
TWCA	Teledyne Wah Chang.
TRB	Timken Roller Bearing Co.
UT	United Technologies Corp.
UCAR	Union Carbide Corp.
Wesgo	Western Gold and Platinum Co.
w	Wrought.

☆U.S. GOVERNMENT PRINTING OFFICE: 1978-603-002/120

50272-101

REPORT DOCUMENTATION PAGE

1\. REPORT NO.
BuMines RI 8335

2\.

3\. Recipient's Accession No.
PB293308

4\. Title and Subtitle
Erosion Testing of Potential Valve Materials for Coal Gasification Systems

5\. Report Date

6\.

7\. Author(s)
J. S. Hansen, J. E. Kelley, and F. W. Wood

8\. Performing Organization Rept. No.

9\. Performing Organization Name and Address
Albany Metallurgy Research Center
Bureau of Mines, USDI
P.O. Box 70
Albany, Oregon 97321

10\. Project/Task/Work Unit No.

11\. Contract(C) or Grant(G) No.
(C)
(G)

12\. Sponsoring Organization Name and Address
Bureau of Mines, USDI
2401 E Street, NW
Washington, D.C. 20241

13\. Type of Report & Period Covered
Report of Investigations

14\.

15\. Supplementary Notes

16\. Abstract (Limit: 200 words)

In support of its objective to conserve mineral resources by minimizing premature failure of materials, the Bureau of Mines conducted a cooperative study with the U.S. Department of Energy on the erosion and abrasion resistance of hard materials for valves in coal conversion systems. This report describes a newly developed erosion-testing apparatus and presents data on the erosion resistance of over 200 materials. Erosion resistance of most metals was comparatively low. In contrast, ceramics and cermets such as B_4C, WC, SiC, Si_3N_4, and TiB_2, when fabricated to minimize porosity, displayed greater than five times the erosion resistance of metals. Coatings such as boron diffused into Mo and WC, chemical-vapor-deposited TiCN, and electrodeposited TiB_2 were highly erosion resistant if applied in thicknesses ranging from 60 to 75 µm. Erosion resistance of cemented carbides was inversely related to metal binder content. This report was prepared in cooperation with the U.S. Department of Energy.

17\. Document Analysis a. Descriptors

solid particle erosion
erosion
erosion resistance
damage
coal gasification
temperature
metal
ceramics
cermet

b\. Identifiers/Open-Ended Terms

c\. COSATI Field/Group

18\. Availability Statement
Release unlimited by NTIS.

19\. Security Class (This Report)

20\. Security Class (This Page)

22\. Price
A03-A01

ANSI-Z39.18)

See Instructions on Reverse

OPTIONAL FORM 272 (4-7
(Formerly NTIS-35)
Department of Commerce